

LA-UR- *12-00642*

Approved for public release;
distribution is unlimited.

Title: Performance optimization of bundled fiber optic
displacement sensors

Author(s):
Erik A. Moro, INST-OFF
Michael D. Todd, UCSD
Anthony D. Puckett, W-3

Intended for: Intended for publication in SPIE conference proceedings and
presentation at (the same) SPIE conference.



Los Alamos National Laboratory, an affirmative action/equal opportunity employer, is operated by the Los Alamos National Security, LLC for the National Nuclear Security Administration of the U.S. Department of Energy under contract DE-AC52-06NA25396. By acceptance of this article, the publisher recognizes that the U.S. Government retains a nonexclusive, royalty-free license to publish or reproduce the published form of this contribution, or to allow others to do so, for U.S. Government purposes. Los Alamos National Laboratory requests that the publisher identify this article as work performed under the auspices of the U.S. Department of Energy. Los Alamos National Laboratory strongly supports academic freedom and a researcher's right to publish; as an institution, however, the Laboratory does not endorse the viewpoint of a publication or guarantee its technical correctness.

Performance optimization of bundled fiber optic displacement sensors

Erik A. Moro ^{*a,b}, Michael D. Todd^a, Anthony D. Puckett^b

^aUniversity of California San Diego, 9500 Gilman Drive, La Jolla, CA, USA 92093;

^bLos Alamos National Laboratory, P.O. Box 1663, Los Alamos, NM, USA 87545

ABSTRACT

Bundled intensity-modulated fiber optic displacement sensors offer high-speed (kHz-MHz) performance with micrometer-level accuracy over a broad range of axial displacements, and they are particularly well-suited for applications where minimally invasive, non-contacting sensing is desired. Furthermore, differential versions of these sensors have the potential to contribute robustness to fluctuating environmental conditions. The performance limitations of these sensors are governed by the relationship between axial displacement and measured power at the locations of receiving fibers within a bundled probe. Since the propagating transmission's power level is spatially non-uniform, the relative locations of receiving fibers within a bundled probe are related to the sensor's output, and in this way fiber location is related to sensor performance.

In this paper, measured power levels are simulated using a validated optical transmission model, and a genetic algorithm is employed for searching the intensity-modulated bundled displacement sensor's design space for bundle configurations that offer high-overall combinations of desired performance metrics (e.g., linearity, sensitivity, accuracy, axial displacement range, etc...). The genetic algorithm determines arrangements of fibers within the bundled probe that optimize a performance-based cost function and have the potential to offer high-performance operation. Multiple converged results of the genetic algorithm generated using different cost function structures are compared. Two optimized configurations are prototyped, and experimental sensor performance is related to simulated performance levels. The prototypes' linearity, sensitivity, accuracy, axial displacement range, and sensor robustness are described, and sensor bandwidth limitations are discussed. This paper has been approved by Los Alamos National Laboratory for unlimited public distribution (LA-UR XX-XXXXXX).

Keywords: Displacement sensor, fiber optic, performance optimization

1. INTRODUCTION AND BACKGROUND

Optical fiber displacement sensors offer advantages over traditional, electromechanical sensing methodologies, such as not being spark sources, being minimally invasive (in some cases not necessitating physical contact), and being immune to electromagnetic interference. In comparison to interferometric displacement sensing approaches, intensity-modulated fiber optic displacement sensors offer reduced complexity (e.g., hardware, environmental control, demodulation, etc...), increased sampling rates, but reduced accuracies. The simplest intensity-modulated fiber optic displacement sensors are two-fiber optical levers [1]. Fundamentally, the displacement of some device-under-test (DUT) results in changes in the amount of light that is collected by receiving fibers, and DUT displacement is related to one or more measured optical power levels (Figure 1). Bundled intensity-modulated displacement sensors include multiple receiving fibers and offer increased sensitivity by gathering an increased percentage of the transmitted electromagnetic signal [2]. Differentially interrogated, bundled intensity-modulated displacement sensors offer increased robustness to fluctuating environmental or hardware conditions [3],[4].

The spatial distribution of the reflection from the DUT (Figure 1) is non-uniform, and the relationship between axial displacement and measured power varies as a function of radial offset. Therefore, a bundled displacement sensor's performance is dictated by the arrangement of optical fibers within the bundle, and in the case of differential sensors, performance depends on the assignment of receiving fibers to one of two receiving groups. Bundle architectures have historically been designed from a limited design space; considering only specific configurations such as the two-concentric ring approach [3] or the random-packing approach [5], and thereby constraining any resulting sensors to limited performance-spaces. Recently, the authors' proposed the use of a genetic algorithm to optimize the arrangement

^{*}eamoro@lanl.gov

of fibers within a bundled probe, according to a particular set of performance-metrics, in an effort to exploit previously unconsidered regions of the sensor's design space and achieve performance-levels that met application-specific demands [6]. The differentially-interrogated, optimized prototype reported by the authors offered a high-overall combination of sensitivity and accuracy over an application-specific linear displacement range, although it showed a lack of robustness to large ($>10\%$) changes in transmitted power level. It was explained in this work that this lack of robustness resulted directly from the use of an optimization cost function that did not include robustness as a performance-metric (i.e., sensor robustness was an assumed byproduct of differential interrogation). In this paper, a second iteration of a differential, optimized prototype is proposed, manufactured, and experimentally tested in an effort to combine high-sensitivity and high-accuracy, over an axial displacement range of 3.5-5.5 mm, while also offering robust performance. The results of this second-iteration optimization routine pose a set of lessons learned regarding the fundamental limitations of sensor performance and the sensitivity of the sensor's output to variability in input parameters.

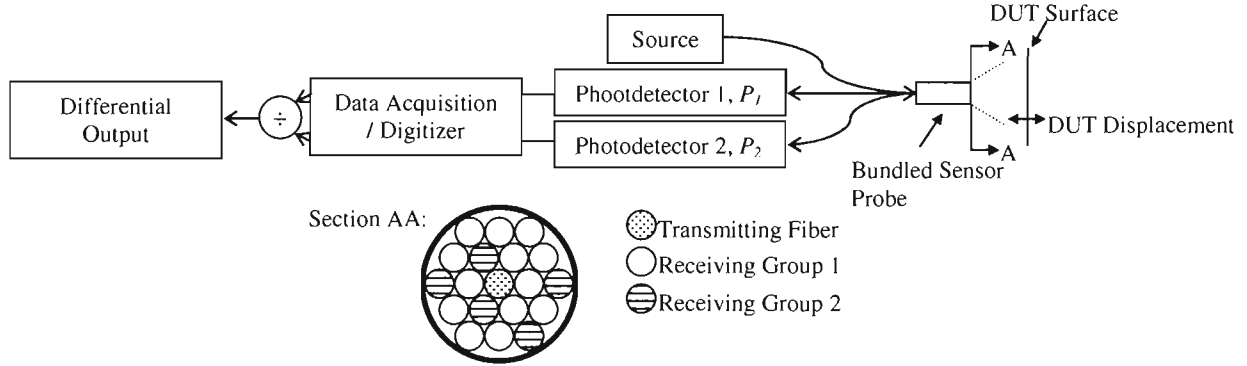


Figure 1. A generic diagram illustrates the key components of a differential, bundled, non-contacting fiber optic displacement sensor. The measurement of multiple receiving groups enables differential sensing, which enhances sensor robustness to some environmental and hardware fluctuations.

2. OPTIMIZATION STRATEGY

The first attempt by the authors at bundle configuration optimization is described in [6]. In this second iteration optimization attempt, the authors employed a strategy that takes a displacement sensor's bundle configuration, as shown in Figure 2, and assigns the 54 receiving fibers to one of two measurement groups for differential displacement measurement. An axial-displacement range of 3.5-5.5 mm, specifically, was targeted, and with a low-power source (<5 mW) additional receiving fibers (beyond the 54 fibers shown in Figure 2) would not have received an appreciable signal level at these ranges. Four differential sensor outputs were considered during optimization: P_1/P_2 , P_2/P_1 , $(P_1-P_2)/(P_1+P_2)$, and $(P_1+P_2)/(P_1-P_2)$.

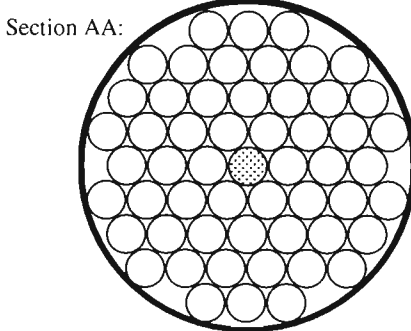


Figure 2. The bundle architecture assumed during optimization is hexagonal close-packed. The centrally-located fiber is assumed to function as the transmitting fiber, and the remaining 54 fibers are assigned to one of two receiving groups in an effort to optimize sensor performance. "Section AA" refers to the cross-section in Figure 1.

A genetic algorithm was employed for searching the bundle's design space, in search of configurations that maximized the cost function

$$Cost = a|S| - (bE)^B - cR. \quad (1)$$

S is the sensor's sensitivity and is calculated as the slope of the output versus axial displacement curve (calculated in mW/mW*mm), E is the linear-modeling error (in %) and is calculated as the maximum absolute error (normalized by the output range) between the sensor output and a linear least-squares fit of the output data, and R is the root-mean-square error (in %) between the nominal linear least-squares fit and a linear least-squares fit (also normalized by the output range) calculated when the transmitted power level is reduced to 40% of nominal. 60% simulated reductions in the transmitted power level account for significant reductions in either the transmission level or (more likely) changes in DUT surface reflectivity, and it was shown in previous work that sensor robustness hinges on P_1 and P_2 being affected identically by changes in transmission power levels [6]. The cost function weights (in Equation (1)) $a=5$, $b=200$, $c=50$ and $B=3$ were chosen by trial-and-error, with the goal of maximizing sensitivity and keeping linear modeling error and robustness error each below 5%. In other words, although high-sensitivity was desired, its utility is limited if the sensor output's deviation from linearity is too large (in this case, defined as greater than 5%). The resulting optimized configuration is shown in Figure 3 with the differential sensor output being measured as $(P_1+P_2)/(P_1-P_2)$. This design is intuitive: the numerator is large, the denominator is small, and since P_1 and P_2 are close in magnitude, they both scale similarly with reductions in the transmitted (or reflected) power level. This sensor was prototyped by an external third party, and a photograph of the actual, prototyped bundle is shown in Figure 4. Obvious discrepancies exist between the assumed hexagonal close-packing (Figure 3) and the actual packing (Figure 4), and their impact will be discussed in detail in Section 4.

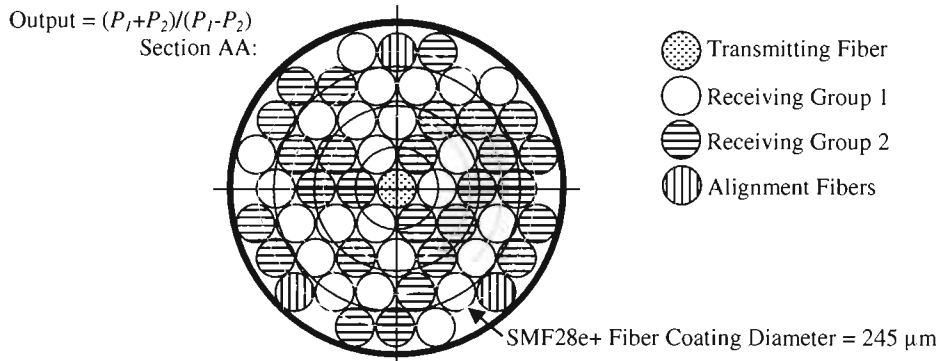


Figure 3. The simulation's optimized configuration is shown. Concentric circles show the radii at which receiving fibers are located. "Section AA" refers to the cross-section in Figure 1. Alignment fibers were used during experimentation, with equal their measured power levels indicating alignment with the DUT.

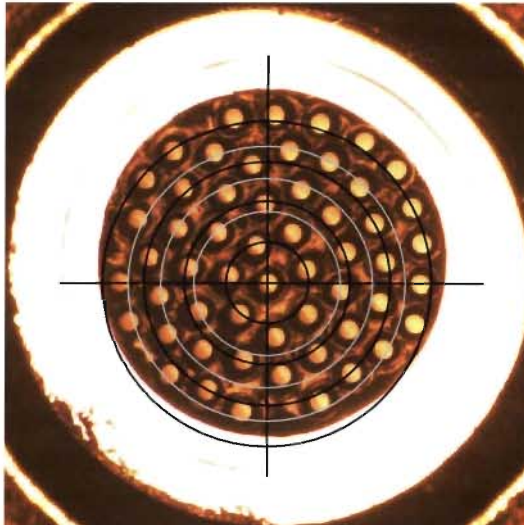


Figure 4. The photograph of the actual prototype bundle is shown here. For reference, axes and concentric circles (corresponding to those shown in Figure 3) are drawn centered at the transmission fiber.

The simulated sensor performance, shown in Figure 5, show a relatively large sensitivity ($0.043 \text{ mW/mW}/\mu\text{m}$), with a low linear modeling error (3.1%), over the prescribed 3.5-5.5 mm axial displacement range. Further, a 60% reduction in the transmitted power level results in only slight (1.1%) deviations to the linear least-squares fit, predicting that the sensor should have strong robustness to changes in surface reflectivity of up to 60%. This robustness, in theory, is derived from the notion that changes in the transmitted power level and changes in surface reflectivity will ultimately be manifested in the same way in both the numerator term (P_1+P_2) and denominator term (P_1-P_2). This compares to the first iteration (non-robust) optimized configuration which offered a sensitivity of $-0.066 \text{ mW/mW}/\mu\text{m}$ with 11% nonlinearity error over an axial displacement range of 6-8 mm [6].

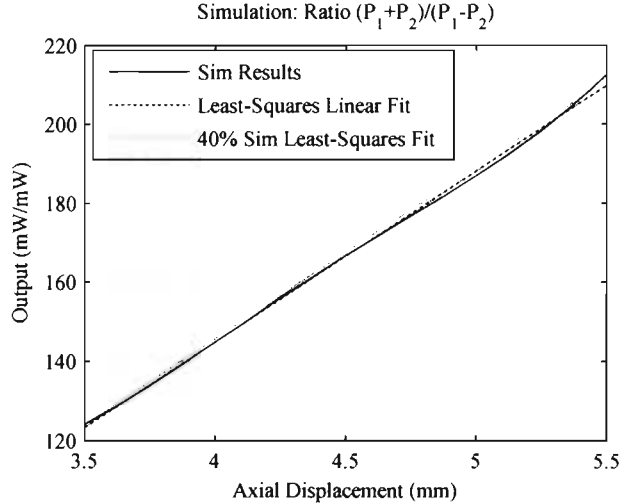


Figure 5. The simulated sensor output is shown for the optimized bundle configuration as a function of axial displacement. A Least-squares linear fit of the simulated data provides an indication of the linearity of the output, and a similar least-squares linear fit is generated assuming a 40% reduction in the transmission's power level.

3. EXPERIMENT

In order to characterize the relationship between sensor output and DUT displacement, the optimized prototype was clamped and aligned with the DUT (Figure 6). The optical source was a thermo-electrically controlled 5 mW superluminescent diode, whose broadband transmission is centered near 1528 nm (Covega Corp. SLD 1108). The DUT was a front-surface silver coated mirror (Thorlabs, Inc., PF10-03-P01) with a percent reflectivity at 1550 nm of about 98%. The DUT position was controlled using a tri-axial linear stage with micrometer accuracy (Newport Corp. 561D). Single mode step index fibers (Corning, Inc. SMF-28e+) were used in the bundled sensor. Broadband InGaAs photodetectors with large (1 mm^2) detection areas (Thorlabs, Inc. DET10C) and a data acquisition system (National Instruments Corp., NI PXI-4461) converted the measured optical signals to digitized, electrical signals. This system had a maximum sampling rate of 200 kHz, limited by the particular data acquisition system employed. With a load resistance of $10 \text{ k}\Omega$, the photodetectors have a bandwidth of 400 kHz, and this may be increased by decreasing the load resistance. 4 dB of attenuation was estimated (experimentally) between the optical source and the data acquisition system. The coupler between the source and the bundled probe has 2 dB of attenuation in and of itself, and it is not unrealistic to attribute 2 dB of attenuation to the bundled package.

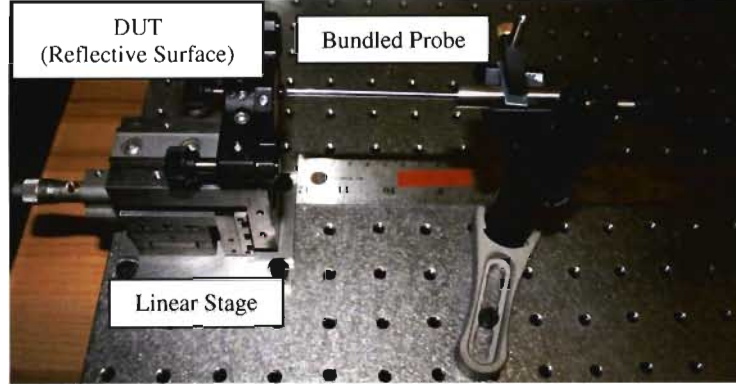


Figure 6. A photograph of the experimental setup is shown here.

4. RESULTS AND DISCUSSION

4.1 Comparison between Experimental and Simulation Results

A comparison of simulated and experimental power measurements P_1 and P_2 (as designated in Figure 1 and Figure 3) is shown in Figure 7, with the experimental data being sampled at a rate of 1 kHz. Two points of agreement between experimental data and simulation data may be observed — (1) P_1 is generally larger than P_2 and (2) both P_1 and P_2 tend to increase as the axial displacement of the DUT is increased from 3.5 mm to 5.5 mm. However, there are also two distinct discrepancies between experimental and simulated results that should be discussed. First, and most significantly, the magnitude of the simulated power measurements is as much as 125% of the experimentally observed magnitude over the 3.5-5.5 mm range. Judging from the discussion in Section 2, this is likely attributed to discrepancy between the predicted bundle packing (true hexagonal close-pack shown in Figure 3) and the actual bundle packing (a less-than-perfect attempt at hexagonal close-packing shown in Figure 4). Deviation from hexagonal close-packing necessarily results in a reduction in fiber density, and this is readily apparent with the actual packing of the prototype (Figure 4). Consequently, one can, at the very least, expect the experimentally measured power levels to be less than simulated (anticipated) ones. A sensitivity analysis is performed in the following subsection in an effort to further characterize the relationship between uncertainty in receiving fiber locations and variability in the observed sensor output. The second readily apparent discrepancy between experiment and simulation is the noise level on P_1 and P_2 . While the magnitude of the noise floor was assumed during the optimization routine (Section 2), the signal to noise ratio (SNR) of the measured data was not considered. Noise on P_1 and P_2 introduces a peaky behavior, which is especially large in comparison to the magnitude of the difference $P_1 - P_2$. When this difference term is put in the denominator of the sensor output, the peaks are amplified, resulting in erratic behavior (Figure 8).

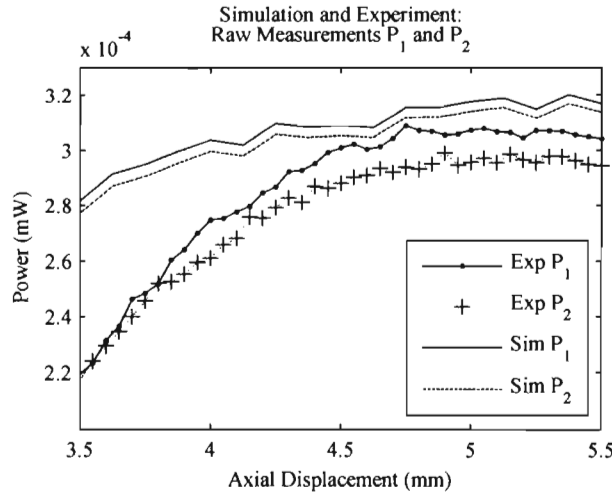


Figure 7. Simulated and experimental power measurements (P_1 and P_2) have a similar shape, although the simulated power levels are generally larger in magnitude.

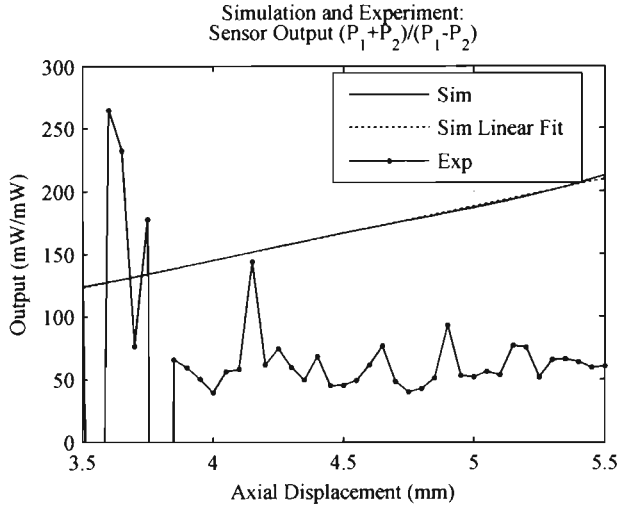


Figure 8. A comparison of experimental and simulated sensor output data shows poor agreement, which can be attributed to reduced fiber density within the bundle and low SNR in P_1 and P_2 .

Recall from Section 2 that this sensor was designed to exhibit high-sensitivity between its output and changes in DUT displacement, but in actuality, it exhibits high-sensitivity to any fluctuations in P_1 and P_2 (and it was previously assumed that these fluctuations would primarily be displacement-related). Unfortunately, detector noise and data acquisition system noise ultimately result in a low sensor SNR, which fundamentally limits the performance of this low-power displacement sensor. The optimization routine did what was “asked” of it in that a sensor with high-sensitivity was designed with an allowable degree of nonlinearity over a prescribed axial displacement range. The magnitude of the noise floor was considered as it pertained to the magnitudes of P_1 and P_2 , since robustness hinges on these terms responding in the same way to variability (e.g., changes in surface reflection, transmitted power level, etc.). However, the optimization routine did not consider overall signal-to-noise ratio along with the fact that, high-sensitivity to axial displacement has in actuality a high sensitivity to perturbations on the sensor input (i.e., measured power level). The end result in this case is high-sensitivity to noise on the measured power levels (manifested either in the photodetectors or the data acquisition system, Figure 1). To rectify this issue, the optimization cost function needs to be re-structured to consider the final SNR of measured signals in addition to the magnitude of the noise floor as it pertains to large (e.g., 40%) reductions in surface reflectivity.

4.2 Sensitivity Analysis

The authors performed a sensitivity analysis of the transmission model for a signal emitting from a step-index, single mode optical fiber [7]. In this analysis, variability in the radial offset between a transmitting fiber and a receiving fiber was shown to largely impact the measured power level. In particular, for this sensor, small changes in the output’s denominator term ($P_1 - P_2$) may result in large changes in the measured sensor output, thereby amplifying the already sensitive relationship between P_1 and P_2 and the true positioning of receiving fibers. A sensitivity analysis is performed by perturbing a model’s input parameter (in this case, the radial offset between transmitting and receiving fibers) in such a way as to thoroughly cover some realistic parameter space, and then observing the variability that results on an output parameter. In this case, the received power levels at particular radial offsets were allowed to vary (according to a uniform distribution) between 80% of nominal and 120% of nominal. This 40% range realistically accounts for deviations in the actual location of receiving fibers as well as the reduced density of receiving fibers, and the assumption of a uniform distribution assumes no prior knowledge (thereby acting as a conservative, first-order estimate). The input parameter variability in this case admittedly will not accurately reflect the actual variability seen in the prototype, but it is useful for showing the highly-sensitive relationship between input parameter variability and sensor output variability. The results of this analysis are shown in Figure 9, where the 25%-quantile and the 75%-quantile of the variable sensor output data are shown in comparison to the observed, experimental sensor output data. Note that these quantiles are calculated assuming no additional noise, and therefore are the direct result of variability in the receiving fiber locations.

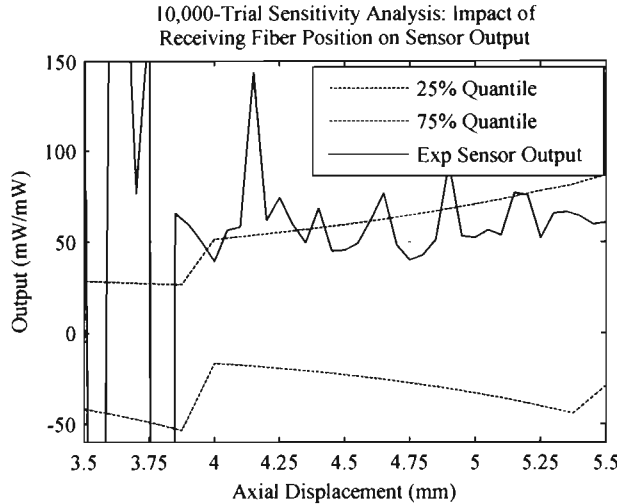


Figure 9. Sensitivity analyses show the dependence that the sensor's output has on the particular location (and bundling) of receiving fibers. In this analysis, variability in fiber position was simulated using variations on the measured power levels, uniformly distributed between 80% and 120% of nominal.

5. CONCLUSION

The authors proposed an optimization framework for use in designing bundled fiber optic displacement sensors whose specific bundling configurations are designed for optimal performance over a prescribed, application-specific displacement range and with an allowable degree of error. The use of a complicated bundling strategy was employed in this paper in hopes of achieving high-overall combinations of sensitivity, accuracy, and linear-displacement range, while maintaining high sampling-rates. This work is part of a larger effort to characterize the performance limitations of intensity-modulated displacement sensors in the presence of some degree of experimental uncertainty, as a basis for comparison to other non-contacting fiber optic sensing methodologies.

The primary shortcoming of the particular sensor investigated in this paper was the difference between the optimally-prescribed (hexagonal close-packed) bundle structure and the actual (prototyped) bundle structure. A sensitivity analysis showed that the sensor's differential output is highly sensitive to variability in the true location of receiving fibers within the bundle. The other major shortcoming of this particular prototyped sensor is the low SNR of the final, measured signals. The highly sensitive nature of the optimized bundle configuration resulted in a sensor that was highly sensitive to input variations of every type, whether they be noise or actual DUT displacement. In future work, parametric uncertainty should be characterized prior to the optimization process, and sensor robustness to uncertainty (fiber locations, SNR, etc...) must be considered in the cost function in any effort to optimize sensor performance. This effort would be in addition to a consideration of the noise floor magnitude as it relates to sensor robustness (as discussed in [6]).

In spite of these shortcomings, this design framework still holds promise, as a previous optimized prototype showed strong agreement between model and experiment [6]. The lessons learned in this research must be considered in any subsequent implementations of this design framework. Further, this approach still offers the potential for facilitating high-performance sensor operation that suits application-specific needs, offering non-contacting displacement measurement with a non-spark emitting source at high (kHz-MHz) sampling rates.

REFERENCES

- [1] Cook, R. O. and Hamm, C. W., "Fiber optic lever displacement transducer," *Appl. Optics* 18 (19), 3230-3241 (1979).
- [2] Huang, H. and Tata, U., "Simulation, implementation, and analysis of an optical fiber bundle distance sensor with single mode illumination," *Appl. Optics* 47(9), 1302-1309 (2008).

- [3] Suganuma, F., Shimamoto, A., and Tanaka, K., "Development of a differential optical-fiber displacement sensor," Appl. Optics 38 (7), 1103-1109 (1999).
- [4] Zheng, J. and Albin, S., "Self-referenced reflective intensity modulated fiber optic displacement sensor," Opt. Eng. 38 (2), 227-232 (1999).
- [5] <http://www.mtiinstruments.com/products/fiberopticmeasurement.aspx>
- [6] Moro, E. A., Todd, M. D., Puckett, A. D., "Using a validated transmission model for the optimization of bundled fiber optic displacement sensors," Appl. Optics 50 (35), 6526-6535 (2011).
- [7] Moro, E. A., Todd, M. D., Puckett, A. D., "Experimental validation and uncertainty quantification of a single-mode optical fiber transmission model," J. of Lightwave Technol. 29 (6), 856-863 (2011).